BEM AND SHEAR LAG METHOD FOR INTERFACE PROBLEM OF BI-MATERIAL STRUCTURE UNDER STATIC LOADING

VARBINKA VALEVA
JORDANKA IVANOVA

Institute of Mechanics, Sofia, Bulgaria

e-mail: valeva@imbm.bas.bg; ivanova@imbm.bas,bg

BARBARA GAMBIN

Institute of Fundamental Technological Research, Warsaw, Poland

e-mail: bgambin@ippt.gov.pl

The behaviour of the interface of a pre-cracked bi-material ceramic-metal structure under static axial loading is an object of interest in the present paper. To solve the problem for interface delamination of the structure and to determine the debond length along the interface, a 2D BEM code was created and applied. The interface plate is assumed as a very thin plate comparing with the others two. The parametric (geometric and elastic) analysis of the debond length and interface shear stress is done. First, the obtained numerical results are compared with analytical ones from 1D Shear lag analysis of the considered structure. The respective comparison is illustrated in figures and shows a good agreement. The comparison between the calculated using 2D BEM code elastic-brittle debond lengths with Song's experimental data for the bi-material structure Zinc/Steel as well as with respective results from FEM simulation shows good coincidence.

Key words: BEM, Shear lag analysis, bi-material structure, debond length

1. Introduction

The boundary element method (BEM) have been demonstrated to be a viable alternative to the FEM for many engineering problems, due to its features of boundary-only discretization and high accuracy (Mukherjee, 1982; Cruse, 1988; Banerjee, 1994). The high accuracy and efficiency of the BEM for stress analysis, especially in fracture mechanics (Cruse, 1988), is very well

recognised of its semi-analytical nature. The meshing for the BEM is also much more efficient than those in other domain-based methods, especially for problems with changing boundaries such as crack propagation problems. Recently, it was shown in liu (1998), both analytically and numerically, that the conventional boundary integral equation can be successfully applied to thin structures, such as layered structures, thin films and coatings. It was shown in Luo *et al.* (1998) that very accurate numerical solutions can be obtained for thin structures with the thickness-to-length ratio in the micro- and even nanoscales, using the newly developed BEM approach, without seeking refinement of the BEM mesh as the thickness decreases.

The interface strength, toughness and stiffness are important factors affecting the mechanical response of multi-material layered structures. A weak interface induces loss of structure stiffness and strength. On the other hand, a brittle and strong interface may induce excessive cracking of bonded elements. Interfacial fracture of layered composite materials under mechanical loading was analysed in numerous papers (see, for example Hutchinson and Suo, 1992). In most papers, the analysis of thin layer cracking combined with progressive delamination is based on assumptions of the linear fracture mechanics. Such behaviour is treated as a mixed mode crack propagation with critical conditions expressed in terms of stress intensity factors (Chiang, 1991; Lemaitre *et al.*, 1996; Zhang, 2000). The crack singularities at bi-material interfaces were analysed by Hw and Hutchinson (1989), Sternitzke *et al.* (1996). The present literature review is not complete as the extensive research is progressing on multilayer and graded layer systems.

Since Cox (1952) proposed a simple one-dimensional equation for analysing the stress transfer between a fibre and a matrix, the Shear lag approximate analysis has become a tool for stress analysis in composite materials as well as in layered structures. The main idea of the Shear lag analysis is such an assumption which involves a simplification of the in-plane shear stress τ_{xy} and decouples the 2D problem into two 1D ones. Hedgepeth (1961) was the first who applied the Shear lag model to unidirectional composites. In the Shear lag models, the hypothesis that the load is transferred from broken fibres to the adjacent ones by the matrix shear force is stated. Hence, the matrix shear force is independent of the transverse displacements. In Ivanova *et al.* (2006), Nikolova *et al.* (2007, 2009), Nikolova (2008), the Shear lag approach was applied to a bi-material layered structure with a pre-cracked first thin layer. Different loadings were considered: static, thermal and combined thermo-mechanical ones. The elastic-brittle, sleep and cohesive behaviour of the interface was assumed and the respective lengths of delamination were found.

The present paper is aimed at the behaviour of the interface of bi-material ceramic-metal plates under static axial load. The interface plate is assumed as a very thin plate comparing with the second one and is subject only to shear stress. To validate the application domain of the Shear lag analysis, the problem for delamination of the interface of the biomaterial structure, a BEM code has been created and used. The numerical model of the structure is considered in a 2D plane-strain state. Delamination starts at the assumed restrict condition for the value of shear stress of the interface. The obtained numerical results are compared with analytical ones from 1D Shear lag analysis, which can give a clear picture of the application of 1D Shear lag analysis. The second comparison between the calculated using 2D BEM code elastic-brittle debond length with Song's experimental data for bi-material structure Zinc/Steel as well as with respective results from FEM simulation (Song *et al.*, 2006) shows good agreement.

2. Shear lag analysis

Consider two elastic plates A and B with finite lengths $2L$, thicknesses $2h_A$, $2h_B$, bonded by an interface I and tensionally loaded with a strain ε_0, and the zero thickness interface undergoing pure shear (Fig. 1). The modified Shear lag model will be applied (Ivanova *et al.*, 2006), taking into account plasticity and damage of the interface. In the shear lag model, negligence of the bending effects results in qualitative values of the stress-strain behaviour. The main purpose of this study is to give simple analytical solutions, helping the design of graded materials.
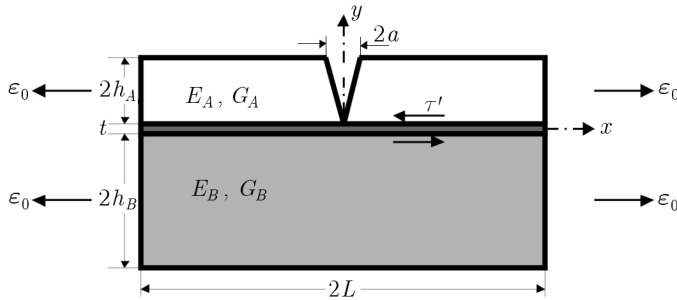

Fig. 1.

The posed problem consists in the following. A crack normal to the interface in the layer A has reached the interface by propagation in mode I. We will

study the conditions for the crack to reinitiate in the layer B. We assume that the conditions of debonding of the interface (mode II) occur before the conditions for crack reinitiation (mode I) in the layer B. The debonding length l will be defined as the length of the interface for which the shear stresses at the interface I reach their critical value for the interface material.

The interface is supposed to be with a negligible thickness and the shear modulus G, shear stress $\tau^I(x,t)$, where the superscript I for stresses and displacement belongs to the interface. It is assumed that the layers and interface are modeled as isotropic elastic materials.

The axial stresses and strains are uniform over the cross section of each plate, working only on tension-pressure, while the interface works on shear. The bending is neglected.

The origin of the Cartesian coordinate system is located at the artificial crack tip. Due to the symmetry, a half of the structure will be considered. The stress-strain behaviour of the structure is determined by $\sigma_i(x)$, $\tau^I(x)$, $\varepsilon_i(x)$, $u_j(x)$ $(i = A, B)$, $(j = A, B, I)$, where by the subscript I we denote the interface displacement $u_I(x)$. The superscript (e) for $\sigma_i(x)$, $\varepsilon_i(x)$, $u_j(x)$ denotes that the elastic law is assumed to describe the interface behaviour.

The following ordinary equilibrium differential equations hold

$$\frac{d\sigma_A^e}{dx} = \frac{\tau^I}{2h_A} \qquad \frac{d\sigma_B^e}{dx} = -\frac{\tau^I}{2h_B} \qquad (2.1)$$

together with respective boundary conditions and constitutive equations.

In this case, the following boundary conditions and constitutive equations for the interface are taken

$$\sigma_A^e(0) = 0 \qquad \varepsilon_A^e(L) = \varepsilon_0 \qquad \varepsilon_B^e(L) = \varepsilon_0$$

$$u_B^e(0) = 0 \qquad u_I^e(0) = u_A^e(0)$$

$$\sigma_A^e(x) = E_A \varepsilon_A^e(x) \qquad \sigma_B^e(x) = E_B \varepsilon_B^e(x) \qquad (2.2)$$

$$\tau^I(x) = G w_E^e(x) \qquad w_I^e(x) = \frac{u_A^e(x) - u_B^e(x)}{h_A + h_B} = \frac{u_I^e(x)}{h_A + h_B}$$

Introduce now non-dimensional parameters, as follows

$$(h_A + h_B)\overline{x} = x \qquad (h_A + h_B)\overline{u}_i^e = u_i^e \qquad E_B \varepsilon_0 \overline{\sigma}_i^e = \sigma_i^e$$

$$E_B \varepsilon_0 \overline{\tau}^I = \tau^I \qquad E_B \varepsilon_0 \overline{G} = G \qquad \varepsilon_0 \overline{\varepsilon}_i^e = \varepsilon_i^e$$

$$\xi = \frac{h_A}{h_B} \qquad \eta = \frac{E_A}{E_B} \qquad i = A, B, I \qquad (2.3)$$

then (2.1), (2.2) become

$$\frac{d\overline{\sigma}_A^e}{d\overline{x}} = \overline{\tau}^I \frac{1+\xi}{2\xi} \qquad\qquad \frac{d\overline{\sigma}_B^e}{d\overline{x}} = -\overline{\tau}^I \frac{1+\xi}{2} \qquad\qquad (2.4)$$

and

$$\overline{u}_I^e(0) = u_A^e(0) \qquad \overline{u}_B^e(0) = 0 \qquad \overline{\varepsilon}_A^e(\overline{L}) = \overline{\varepsilon}_B^e(\overline{L}) = 1$$

$$\overline{\sigma}_A^e(0) = 0 \qquad \overline{\sigma}_A^e(\overline{x}) = \eta\overline{\varepsilon}_A^e(\overline{x}) \qquad \overline{\sigma}_B^e(\overline{x}) = \overline{\varepsilon}_B^e(\overline{x}) \qquad (2.5)$$

$$\overline{\tau}^I(\overline{x}) = \overline{G}\overline{u}_I^e(\overline{x})$$

Equations (2.4) result in

$$\frac{d^2\overline{u}_I^e}{d\overline{x}^2} = \overline{\lambda}^2 \overline{u}_I^e \qquad\qquad (2.6)$$

where

$$\overline{\lambda}^2 = \frac{\overline{G}(1+\xi)(1+\xi\eta)}{2\xi\eta}$$

and (2.4) becomes

$$\frac{d^2\overline{u}_A^e}{d\overline{x}^2} = \frac{\overline{\lambda}^2}{1+\xi\eta}\overline{u}_I^e \qquad\qquad \frac{d^2\overline{u}_B^e}{d\overline{x}^2} = -\frac{\overline{\lambda}^2}{1+\xi\eta}\xi\eta\overline{u}_I^e$$

The general solution to (2.6) is

$$\overline{u}_I^e(\overline{x}) = A_1 \sinh(\overline{\lambda}\overline{x}) + A_2 \cosh(\overline{\lambda}\overline{x}) \qquad\qquad (2.7)$$

To find the stresses, strains and respective displacements in the plates, we use equations (2.4), together with boundary conditions (2.5). In addition, the substitution $u_I^e(x) = u_A^e(x) - u_B^e(x)$ has to be made.

We obtain the following expressions for the interfacial displacement and shear stress in dimensionless parameters

$$\overline{u}_I^e(\overline{x}) = \frac{1+\xi\eta}{\overline{\lambda}}\frac{\cosh[\overline{\lambda}(\overline{L}-\overline{x})]}{\sinh(\overline{\lambda}\overline{L})} \qquad\qquad \overline{\tau}^I(\overline{x}) = \overline{G}\frac{1+\xi\eta}{\overline{\lambda}}\frac{\cosh[\overline{\lambda}(\overline{L}-\overline{x})]}{\sinh(\overline{\lambda}\overline{L})} \quad (2.8)$$

The debond length $\overline{l}_e$, which gives the magnitude of brittle cracking along the interface can be calculated from (2.8) on the assumption that the shear stress reaches its critical failure value $\overline{\tau}^I = \overline{\tau}^{cr}$ and $\overline{u}_I^e(\overline{l}_e) = \overline{u}^{cr} = \overline{\tau}^{cr}/\overline{G}$. Then

$$\overline{\tau}^{cr} = \overline{G}\frac{1+\xi\eta}{\overline{\lambda}}\frac{\cosh[\overline{\lambda}(\overline{L}-\overline{l}_e)]}{\sinh(\overline{\lambda}\overline{L})} \qquad\qquad (2.9)$$

Using the substitution $\exp[\overline{\lambda}(\overline{L} - \overline{l}_e)] = y$ and (2.9), the following equation for y is obtained

$$y^2 - 2Ay + 1 = 0 \qquad A = \frac{\overline{\lambda}\overline{\tau}^{cr}\sinh(\overline{\lambda L})}{\overline{G}(1 + \xi\eta)} \qquad (2.10)$$

Then two roots of (2.10) are available: $y_{1,2} = A \pm \sqrt{A^2 - 1}$. Now using the substitution $\exp[\overline{\lambda}(\overline{L} - \overline{l}_e)] = y$, we obtain

$$(\overline{l}_e)_{1,2} = \overline{L} - \frac{1}{\overline{\lambda}}\ln[A \pm \sqrt{A^2 - 1}]$$

It is necessary that

$$A^2 - 1 = \Big[\frac{\overline{\lambda}\overline{\tau}^{cr}\sinh(\overline{\lambda L})}{\overline{G}(1 + \xi\eta)}\Big]^2 - 1 > 0$$

This requirement poses some condition for the value of $\overline{\tau}^{cr}$.

Then we have to choose the length of the debonding zone from a condition that this length must be minimum (Ivanova *et al.*, 2006), i.e.

$$\overline{l}_e = \overline{L} - \frac{1}{\overline{\lambda}}\ln[A + \sqrt{A^2 - 1}] \qquad (2.11)$$

3. BEM formulation

The following known boundary integral equations for two-dimensional elasticity problems can be applied in each material domain (index notation is used, where repeated subscripts imply summation) (Mukherjee, 1982)

$$C_{ij}(P_0)u_j^{(\beta)}(P_0) = \int_{\Gamma}[U_{ij}^{(\beta)}(P, P_0)t_j^{(\beta)}(P) - T_{ij}^{(\beta)}(P, P_0)u_j^{(\beta)}(P)]\, d\Gamma(P) \quad (3.1)$$

in which $u_j^{(\beta)}$ and $t_j^{(\beta)}$ are the displacement and traction fields, respectively; $U_{ij}^{(\beta)}(P, P_0)$ and $T_{ij}^{(\beta)}(P, P_0)$ the displacement and traction kernels (Kelvin's solution), respectively; P is the field point and P_0 – the source point, and Γ – the boundary of the single domain. $C_{ij}(P_0)$ is a constant coefficient matrix depending on the smoothness of the boundary Γ at the source point P_0. The superscript β on the variables in Eq. (3.1) signifies the dependence of these variables on the individual domains $\beta = A, B, I$.

The two kernel functions $U_{ij}^{(\beta)}(P, P_0)$ and $T_{ij}^{(\beta)}(P, P_0)$ in boundary integral equation (3.1) for plain-strain problems are given as follows

$$U_{ij}^{(\beta)}(P, P_0) = \frac{1}{8\pi\mu^{(\beta)}(1 - \nu^{(\beta)})}\Big[(3 - 4\nu)\delta_{ij}\ln\Big(\frac{1}{r}\Big) + r_{,i}\, r_{,j}\Big]$$

$$T_{ij}^{(\beta)}(P, P_0) = -\frac{1}{4\pi r(1 - \nu^{(\beta)})} \cdot$$

$$\cdot\Big\{r_{,n}\Big[\Big(1 - 2\nu^{(\beta)}\Big)\delta_{ij} + 2r_{,i}\, r_{,j}\Big] + \Big(1 - 2\nu^{(\beta)}\Big)(r_{,j}\, n_i - r_{,i}\, n_j)\Big\}$$

(3.2)

where $\mu^{(\beta)}$ is the shear modulus and $\nu^{(\beta)}$ Poisson's ratio for three different domains, respectively; r is the distance from the source point P_0 to the field point P; n_i is the i-th directional cosine of the outward normal n; $(\cdot)_{,i} = \partial(\cdot)/\partial x_i$ with x_i being the coordinate of the field point P; and δ_{ij} is the Kronecker delta.

In Eq. (3.1), the integral containing the $U_{ij}^{(\beta)}(P, P_0)$ kernel is weakly singular, while the one containing $T_{ij}^{(\beta)}(P, P_0)$ is strongly singular and must be interpreted in the Cauchy principal value sense. However, when the structure becomes thin in shape, such as the interphase, both integrals are difficult to deal with when the source point is on the one side and the integration is carried out on the other side of the thin structure. These types of integrals are called nearly singular integrals since the distance r is very small in this case but is still not zero. Recently, several techniques, including singularity subtractions, analytical integration, and nonlinear coordinate transformations have been developed to calculate the nearly singular integrals (Luo *et al.*, 1998). The combination of these techniques is found to be extremely effective and efficient in computing the nearly singular integrals in two-dimensional boundary integral equations, no matter how close the source point to the element of integration is.

The discretization of BIE (3.1) using boundary elements follows the standard BEM procedures except for the nearly-singular integrals. For multi-domain (material) problems, the resulting BEM equations for each material domain are coupled together by the interface conditions (continuity of both displacements and equilibrium of both tractions) and then solved to obtain the displacement and traction vectors at each node on the boundary and interfaces. In the BEM approach used in the present paper, for solving the nearly singular integrals, subdivision of the element of integration and an adaptive integration scheme are proposed. For the integration of a logarithmic function, a modified Gauss Quadrature (Gauss-Laguerre) is used. For the case when the collocation point is located at the element or is very close to the element, the

integration of the nonsingular part (where the shape function value is zero at the collocation point) and the singular part (for weakly singular behaviour of the kernel) is performed separately. For the corners, discontinuous elements are used.

4.   Numerical example

The first numerical example is a comparison between the BEM and Shear lag model results.

On the basis of the obtained analytical formulae for the assumed interface shear stress law, the stress behaviour (especially the debond length on the interface) of the two-plate structure with different mechanical and geometric properties under tension ε_0 will be studied. Using BEM, the bending of the structure is avoided by the imposed boundary condition $u_B(x, -(2h_B+t)) = 0$, where t is the thickness of the interface I.

The following geometric and mechanical properties (Table 1) are used:

$$2L = 24\,\text{mm}, \quad 2h_B = 6',\text{mm} \quad \begin{cases} 2h_A = 2\,\text{mm}, & (\xi = 1/3) \\ 2h_A = 1\,\text{mm}, & (\xi = 1/6) \end{cases}$$

$$\tau^{cr} = 18\,\text{MPa}, \quad a = 1\,\text{mm}, \quad t = 0.1\,\text{mm}, \varepsilon_0 \in [0.001, 0.008]$$

Table 1. Characteristics of the materials (Sternitzke *et al.*, 1996)

	Material	E [GPa]	ν [–]
Layer A	C84 [Al$_2$O$_3$/Al composites, (C84=84 vol% Al$_2$O$_3$+16 vol% Al)]	285	0.28
Layer A	Alumina [DEGUSSIT Al 23, Friatec.]	380	0.24
Layer B	100Cr6 [AISI 52100]	210	0.29
Interphase	Polyacrylate thermoplastic glue	2.5	0.50

In Fig. 2, a comparison between 1D Shear lag and BEM 2D interface debond length predictions is shown. The values of debond length l_e versus the applied load ε_0 are obtained for two different ratios η of the elastic moduli and for two different values of the thickness ratio ξ.

It can be seen that geometric characteristics much more influence the debond length than the material characteristics. Considering the numerical and

analytical results (BEM, Shear lag), the bigger is the thickness ratio ξ, the smaller is the value of applied load ε_0^{cr} needed for full delamination (degradation) of the interface. The critical load ε_0^{cr} calculated using Shear lag at different thickness ratios ξ is much smaller comparing with ε_0^{cr} obtained by BEM. This difference for ε_0^{cr} can be explained with the presence of a normal crack, which strongly reflects on the stress-strain behaviour (BEM) of the first plate. On the other hand, the very thin first pre-cracked plate plays a significant role in full degradation of the bi-material structure, allowing for a bigger critical load.
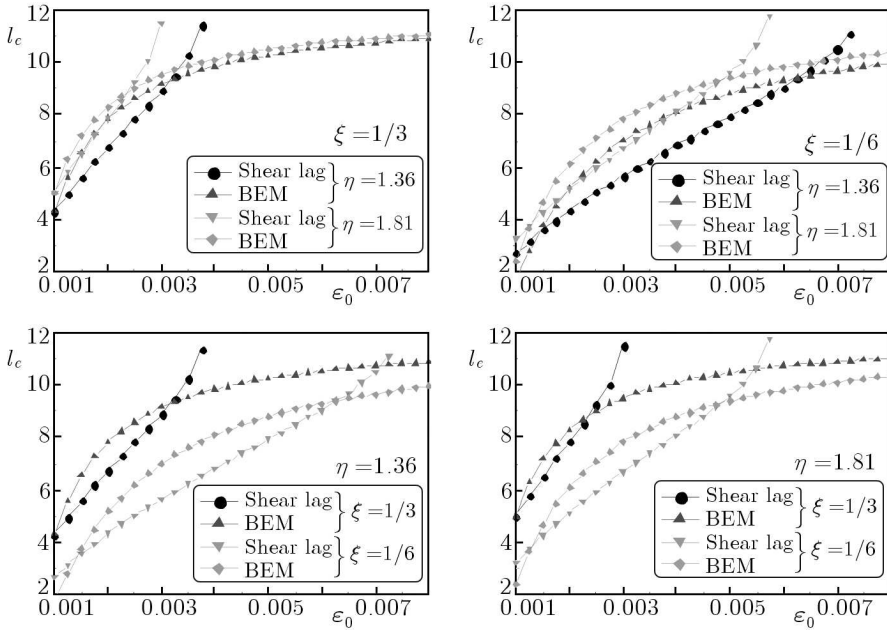

Fig. 2. Comparison and parametric analysis (geometric and elastic properties) between the BEM and Shear lag model for the debond length

The relative error of comparison between the BEM and Shear lag values of the debond length

$$r = \sqrt{\frac{1}{M} \sum_{i=1}^{M} \frac{y_i^{theory}}{y_i^{BEM}}} \cdot 100\%$$

is:

C84/100Cr6		
$\xi = 1/3$	$\eta = 1.36$	$r = 10.75\%$
$\xi = 1/6$	$\eta = 1.36$	$r = 13.01\%$

Alumina/100Cr6		
$\xi = 1/3$	$\eta = 1.81$	$r = 9.22\%$
$\xi = 1/6$	$\eta = 1.81$	$r = 11.64\%$

The investigations show that the bigger is the load, the bigger is the relative error. The decreasing of the thickness of the first plate ξ at a constant elastic ratio η also leads to increment of the relative error. The increasing of the value of the elastic ratio η at a constant value of the geometric ratio ξ leads to decrement of the relative error. It is a consequence of negligible thickness of the interface as well as the fact that the approximate analytical Shear lag model is 1D.

In Fig. 3, the numerical BEM results for stresses of the bi-material structure for $\xi = 1/3$ and $\eta = 1.81$ are shown (as an example). The loading is $\varepsilon_0 = 0.0025$.
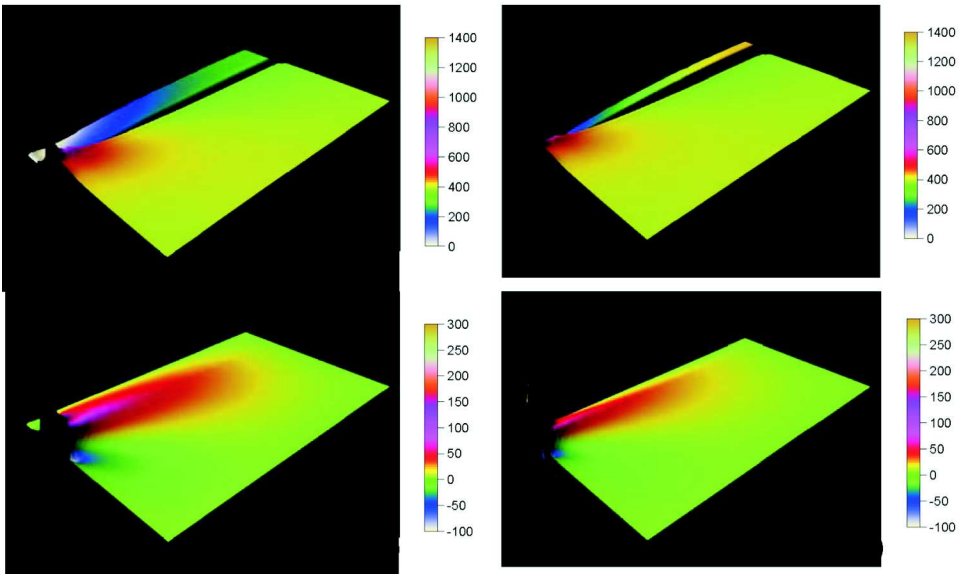

Fig. 3. Plots of stresses $\sigma_{xx}(x,y)$, $\sigma_{xy}(x,y)$ for the pre-cracked bimaterial structure for different thickness ratios $\xi = h_A/h_B$ and the elastic moduli ratio $\eta = 1.81$

The second numerical example is the comparison between the experimental data and FEM results for progressive elastic-brittle interface debond lengths of zinc coatings on a steel substrate (Song *et al.*, 2006) with our BEM results for respective values of debond lengths. The calculations are performed for the following geometrical and mechanical properties of the zinc coating (layer A)

and steel substrate (layer B): $2L = 100\,\mu m$, $2h_A = 10\,\mu m$, $2h_B = 50\,\mu m$, $E_A = 70\,\text{GPa}$, $\nu_A = 0.3$, $E_B = 200\,\text{GPa}$, $\nu_A = 0.27$. The delamination along the zinc coating/steel substrate interface is simulated by deleting the elements for which the shear stress is larger than the critical value representing the interface strength – this is the criterion for crack initiation and propagation along the zinc coating/steel interface with increasing tensile load. Figure 4 shows the interface debond length l_e as a function of the applied strain ε_0, comparing the experimental and calculated by FEM and BEM data for the given interface shear strength of 180 MPa. The BEM results for debond length are in very good coincidence with the experimental data and FEM results by Song *et al.* (2006).
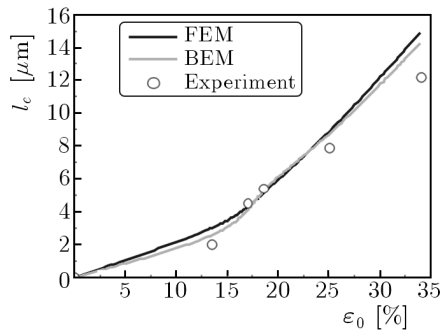

Fig. 4. Measured average interface debond length l_e as a function of the applied strain ε_0 versus calculated interface debond length for the zinc coating shear strength $\tau^{cr} = 180\,\text{MPa}$

5. Conclusions

In the paper, a comparison between the approximate Shear lag 1D method and 2D BEM for interface delamination of the bi-material structure under static load is done. The relative error between analytical and numerical results confirms validity of the Shear lag approach. The obtained predictions can be applied to a pre-cracked by an indentor bi-material structures undergoing static tension for different mechanical behaviour and materials of plates.

References

1. Banerjee P.K., 1994, *The Boundary Element Methods in Engineering*, 2nd ed., McGraw-Hill, New York

2. Chiang R., 1991, On the stress intensity factors of crack near an interface between two media, *Int. J. Fracture*, **47**, R55-R58

3. Cox L.H., 1952, The elasticity and strength of paper and other fibrous materials, *Brit. J. Appl. Phys.*, **72**, 3

4. Cruse T.A., 1988, *Boundary Element Analysis in Computational Fracture Mechanics*, Kluwer Academic Publishers, Dordrecht, The Netherlands

5. He M.Y., Hutchinson J.W., 1989, Crack deflection at an interface between dissimilar elastic materials, *Int. J. Solids Structures*, **25**, 9, 1053-1067

6. Hedgepeth J.M., 1961, *Stress Concentrations in Filamentary Structures*, NASA TN D-882

7. Hutchinson J.W., Suo Z., 1992, Mixed mode cracking in layered materials, *Adv. Appl. Mech.*, **29**, 62-191

8. Ivanova J., Valeva V., Mroz Z., 2006, Mechanical modelling of the delamination of bi-material plate structure, *Journal of Theoretical and Applied Mechanics*, Sofia, **36**, 4, 39-54

9. Lemaitre J., Desmorat R., Vidonne M.P., Zhang P., 1996, Reinitiation of a crack reaching an interface, *Int. J. Fracture*, **80**, 257-276

10. Liu Y.J., 1998, Analysis of shell-like structures by the boundary element method based on 3-D elasticity: formulation and verification, *Int. J. Numer. Methods Engrg.*, **41**, 541-558

11. Luo J.F., Liu Y.J., Berger E.J., 1998, Analysis of two-dimensional thin structures (from micro- to nano-scales) using the boundary element method, *Comput. Mechanics*, **24**, 404-412

12. Mukherjee S., 1982, *Boundary Element Methods in Creep and Fracture*, Applied Science Publisher, New York

13. Nikolova G., 2008, *Thermo-Mechanical Behaviour of Thin Graded Layered Structures*, PhD Thesis

14. Nikolova G., Ivanova J., 2009, Cracked biomaterial plates under thermo-mechanical loading, *Proceedings Fractography of Advanced Ceramics III, Trans. Tech. Publications Ltd. In Key Material Series*, **409**, 406-413

15. Nikolova G., Ivanova J., Valeva V., Mroz Z., 2007, Mechanical and thermal loading of two-plate structure, *Comptes Rendus De L'Academie Bulgare Des Sciences*, **60**, 7, pp. 735

16. Song G.M., Sloof W.G., Pei Y.T., De Hosson J.Th.M., 2006, Interface behaviour of zinc coating on steel: Experiments and finite element calculations, *Surface and Coating Technology*, **201**, 4311-4316

17. Sternitzke M., Knechtel M., Hoffman M., Broszeit E., Rödel J., 1996, Wear properties of alumina/aluminum composites with interpenetrating networks, *J. Am. Ceram. Soc.*, **79**, 1, 121-128

18. Zhang S., 2000, Thermal stress intensities at an interface crack between two elastic layers, *Int. J. Fract.*, **106**, 277-290

Tytuł w j. polskim – proszę dopisać!!

Streszczenie

Streszczenie w j. polskim – proszę dopisać!!